Robust R-D Parameter Estimation via Closed-Form PARAFAC in Kronecker Colored Environments

João Paulo C. L. da Costa [#1], Dominik Schulz [*2], Florian Roemer [*3], Martin Haardt [*4], José A. Apolinário Jr. [#5]

[#] *Department of Electrical Engineering, Military Institute of Engineering (IME), Brazil*
{[1] joaopaulo.dacosta, [5] apolin}@ime.eb.br

[*] *Communications Research Laboratory, Ilmenau University of Technology, Germany*
{[2] dominik.schulz, [3] florian.roemer, [4] martin.haardt}@tu-ilmenau.de

***Abstract*—To estimate parameters from measurements sampled on a multidimensional grid, Parallel Factor Analysis (PARAFAC) based schemes are very appealing, since they are applicable to mixed array geometries, which are a mixture of arbitrary arrays and outer product based arrays. Moreover, for PARAFAC based schemes, errors in some dimensions do not affect the estimation of parameters in the other dimensions. Particularly, the closed-form PARAFAC based parameter estimator has the additional advantage of being non-iterative.**

In this contribution, we propose a PARAFAC decomposition for colored noise with a Kronecker structure called Sequential Generalized Singular Value Decomposition (S-GSVD) based closed-form PARAFAC. Our proposed estimator joins the advantages of the closed-form PARAFAC — such as the applicability to mixed array geometries and the robustness to arrays with positioning errors — with the suitability of the S-GSVD for data contaminated by Kronecker colored noise or interference.

I. Introduction

High-resolution parameter estimation from R-dimensional signals is a task required for a variety of applications, such as estimating the multidimensional parameters of the dominant multipath components from MIMO channels measurements, radar, sonar, seismology, and medical imaging.

As shown in [1], subspace-based parameter estimation schemes, such as the R-D Standard Tensor-ESPRIT [2], can be significantly improved via the Sequential GSVD based prewhitening technique in environments with multidimensional colored noise with Kronecker structure, which is found in some EEG applications [3] as well as in certain MIMO applications [4]. However, ESPRIT-type algorithms [2] are restricted to shift invariant arrays, while, as shown in [5], PARAFAC based parameter estimation schemes, such as the closed-form PARAFAC based parameter estimator, can be applied for mixed array geometries, which are composed of arbitrary arrays and outer product based arrays (OPAs). More details about OPAs can be found in Section II. Moreover, since after a jointly multidimensional data processing the PARAFAC decomposition decouples the dimensions, parameter estimation based on this technique is more robust for scenarios with positioning errors in the arrays [5].

Since the PARAFAC decomposition assumes white noise [6], we propose a PARAFAC decomposition for colored noise called Sequential GSVD [1] based closed-form PARAFAC, where the colored Kronecker noise or interference is taken into account. In our proposed scheme, the Higher Order Singular Value Decomposition (HOSVD) [7] used in closed-form PARAFAC [8] is replaced by the Sequential GSVD [1] of two tensors. By combining the S-GSVD [1] and closed-form PARAFAC [8], we propose a new PARAFAC decomposition and show how to use this new PARAFAC decomposition in parameter estimation problems. The proposed scheme for parameter estimation can be used in mixed array geometries and for arrays with positioning errors as well as in the presence of the Kronecker colored noise or interference.

II. Data model

We consider the superposition of d planar wavefronts captured by an R-D array at N subsequent time instants. In the r-th dimension of the R-D array, there are M_r sensors. Thus, the measurements obey the following model

$$\begin{aligned} \boldsymbol{\mathcal{X}} &= \boldsymbol{\mathcal{I}}_{R+1,d} \times_1 \boldsymbol{A}^{(1)} \ldots \times_R \boldsymbol{A}^{(R)} \times_{R+1} \boldsymbol{S}^{\mathrm{T}} + \boldsymbol{\mathcal{N}}^{(\mathrm{c})} \\ &= \boldsymbol{\mathcal{X}}_0 + \boldsymbol{\mathcal{N}}^{(\mathrm{c})}, \end{aligned} \tag{1}$$

where $\boldsymbol{A}^{(r)} \in \mathbb{C}^{M_r \times d}$ is the array steering matrix in the r-th mode with $r = 1, \ldots, R$, the factor matrix $\boldsymbol{S} \in \mathbb{C}^{d \times N}$ contains the source symbols $s_i(n)$, and in the tensor $\boldsymbol{\mathcal{N}}^{(\mathrm{c})} \in \mathbb{C}^{M_1 \times M_2 \times \ldots \times M_R \times N}$ the colored ZMCSCG (zero-mean circularly-symmetric complex Gaussian) noise samples with variance σ_n^2 are collected. We define $\boldsymbol{\mathcal{I}}_{R+1,d}$ as the identity tensor with $R+1$ dimensions, where each dimension has size d. The elements of $\boldsymbol{\mathcal{I}}_{R+1,d}$ are equal to 1 when all indices are equal and 0 otherwise. The r-th unfolding of $\boldsymbol{\mathcal{A}}$ is represented by $[\boldsymbol{\mathcal{A}}]_{(r)}$ and it is the matrix form of $\boldsymbol{\mathcal{A}}$ varying the r-th index along the rows and stacking all the other indices along the columns of $[\boldsymbol{\mathcal{A}}]_{(r)}$ in the same order as in [7]. In (1) the operator $\times_r$ stands for the r-mode product, which is obtained by multiplying all r-mode vectors by a matrix from the left-hand side and is defined as $[\boldsymbol{\mathcal{A}} \times_r \boldsymbol{U}]_{(r)} = \boldsymbol{U} \cdot [\boldsymbol{\mathcal{A}}]_{(r)}$ according to [7]. The superscript $^{\mathrm{T}}$ stands for transposition and other superscripts used here are $^{\mathrm{H}}$ and $^{-1}$, which mean Hermitian transposition and matrix inversion, respectively. We represent the i-th column of $\boldsymbol{A}^{(r)}$ as $\boldsymbol{a}_i^{(r)}$, which is as function of $e^{j \cdot \mu_i^{(r)}}$, where $\mu_i^{(r)}$ with $r = 1, \ldots, R$ and $i = 1, \ldots, d$ are the spatial frequencies of the i-th source in the r-th dimension. Our objective is to estimate all the spatial frequencies $\mu_i^{(r)}$ from the d dominant components of $\boldsymbol{\mathcal{X}}$ in the presence of

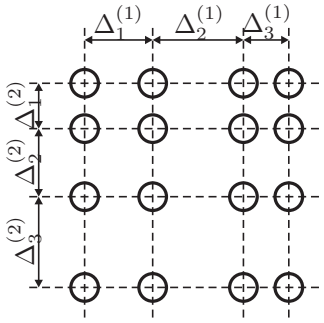

Figure 1. An example of a 2-D outer product based array (OPA) of size 4×4 is illustrated. All the distances $\Delta_i^{(r)}$ for $i = 1, 2, 3$ and for $r = 1, 2$ may assume different values.

colored noise or interference with a Kronecker structure. The model order is assumed to be known. For efficient multi-dimensional model order selection schemes, the reader is referred to [9], [10], [5].

The noiseless tensor $\boldsymbol{\mathcal{X}}_0 \in \mathbb{C}^{M_1 \times M_2 \times \ldots \times M_R \times M_{R+1}}$ in (1) is called an outer product based array (OPA), since it can be written as

$$\boldsymbol{\mathcal{X}}_0 = \sum_{i=1}^{d} \boldsymbol{a}_i^{(1)} \circ \boldsymbol{a}_i^{(2)} \circ \ldots \circ \boldsymbol{a}_i^{(R)} \circ \left(\boldsymbol{s}_i^{(R+1)}\right)^{\mathrm{T}}, \tag{2}$$

where $\circ$ is the outer product operator.

For instance, a 2-D OPA can be formed as an outer product of two uniform linear arrays (ULAs), which gives rise to a uniform rectangular array (URA). On the other hand, the outer product of non-uniform linear arrays (NULAs) is also an OPA, which we refer to as non-uniform rectangular array (NURA). We exemplify a 2-D OPA formed by NULAs in Fig. 1. OPAs with more dimensions are typically present if a sensor array is used to measure a signal at consecutive time instants and/or on a regular grid of frequency bins.

In case of ULAs/URAs, the corresponding array steering vectors have a Vandermonde structure, while NULAs/NURAs can be divided into arrays with shift invariant array steering vectors (where ESPRIT-type methods are applicable), and those without shift invariance. The arrays that are non-outer product arrays are called arbitrary arrays. Note that we also study the impact of calibration errors, which means that the actual sensor positions are not perfectly known.

As shown in [5], the closed-form PARAFAC based parameter estimator (CFP-PE) can be used for Outer Product based Arrays (OPAs). Moreover, the CFP-PE is also applicable for mixed arrays, which have some dimensions as Arbitrary Arrays (AAs) and others as OPAs. Note that physical dimensions that do not possess an outer product structure are represented by a single dimension in our model. For example, a 2-D array without outer product structure is represented by one array steering matrix $\boldsymbol{A}^{(r)} \in \mathbb{C}^{M_r \times d}$, like a 1-D array.

As in [1], the multidimensional colored noise is assumed to have a Kronecker structure, which can be written as

$$\left[\boldsymbol{\mathcal{N}}^{(\mathrm{c})}\right]_{(R+1)} = \boldsymbol{L}_{R+1} \cdot [\boldsymbol{\mathcal{N}}]_{(R+1)} \cdot (\boldsymbol{L}_1 \otimes \boldsymbol{L}_2 \otimes \ldots \otimes \boldsymbol{L}_R)^{\mathrm{T}}, \tag{3}$$

where $\otimes$ represents the Kronecker product, $\boldsymbol{\mathcal{N}} \in \mathbb{C}^{M_1 \times M_2 \ldots \times N}$ is a tensor with i.i.d. ZMCSCG elements, and $\boldsymbol{L}_r \in \mathbb{C}^{M_r \times M_r}$ is a correlation factor of the r-th dimension of the colored noise tensor. Similarly to [1], we can rewrite (3) by using the n-mode products in the following fashion

$$\boldsymbol{\mathcal{N}}^{(\mathrm{c})} = \boldsymbol{\mathcal{N}} \times_1 \boldsymbol{L}_1 \times_2 \boldsymbol{L}_2 \ldots \times_R \boldsymbol{L}_R \times_{R+1} \boldsymbol{L}_{R+1}. \tag{4}$$

The noise covariance matrix in the i-th mode $\boldsymbol{W}_i$ is defined as

$$\mathrm{E}\left\{\left[\boldsymbol{\mathcal{N}}^{(\mathrm{c})}\right]_{(i)} \cdot \left[\boldsymbol{\mathcal{N}}^{(\mathrm{c})}\right]_{(i)}^{\mathrm{H}}\right\} = \alpha \cdot \boldsymbol{W}_i = \alpha \cdot \boldsymbol{L}_i \cdot \boldsymbol{L}_i^{\mathrm{H}}, \tag{5}$$

where α is a normalization constant, such that $\mathrm{tr}(\boldsymbol{L}_i \cdot \boldsymbol{L}_i^{\mathrm{H}}) = M_i$. The equivalence between (3), (4), and (5) is shown in [1], and it is the basis for the S-GSVD [1].

For applications where noise samples without the presence of signal components are not available, the I-S-GSVD can be applied [11].

III. Sequential GSVD based closed-form PARAFAC based parameter estimator (S-CFP-PE)

In this section, we present the proposed PARAFAC decomposition of the tensors $\boldsymbol{\mathcal{X}}$ and $\boldsymbol{\mathcal{N}}^{(\mathrm{c})}$. For the closed-form PARAFAC, the estimation of the factors of the PARAFAC decomposition is transformed into a simultaneous diagonalization problem based on the relation between the truncated HOSVD-based [7] low-rank approximation of $\boldsymbol{\mathcal{X}}$ and the PARAFAC decomposition of $\boldsymbol{\mathcal{X}}$. Here we propose to replace the HOSVD by the S-GSVD of $\boldsymbol{\mathcal{X}}$ and $\boldsymbol{\mathcal{N}}^{(\mathrm{c})}$ in order to obtain a S-GSVD-based [1] closed-form PARAFAC.

As proposed in [1], the S-GSVD is based on the computation of the GSVD of each r-mode unfolding of the tensor $\boldsymbol{\mathcal{X}}$ and of $\hat{\boldsymbol{L}}_r$. The sequential computation of the GSVDs starts with $r = 1$ and the computation in each dimension r can be represented by the tensor $\widetilde{\boldsymbol{\mathcal{X}}}^{(r)}$ as follows

$$\left[\widetilde{\boldsymbol{\mathcal{X}}}^{(r)}\right]_{(r)} = \hat{\boldsymbol{L}}_r^{-1} \cdot \left[\widetilde{\boldsymbol{\mathcal{X}}}^{(r-1)}\right]_{(r)} = \boldsymbol{U}_r^{(L)} \cdot \boldsymbol{\Xi}_r^{(L)^{-1}} \cdot \boldsymbol{\Xi}_r^{(X)^{\mathrm{T}}} \cdot \boldsymbol{U}_r^{(X)^{\mathrm{H}}}, \tag{6}$$

which is equivalent to

$$\widetilde{\boldsymbol{\mathcal{X}}}^{(r)} = \widetilde{\boldsymbol{\mathcal{X}}}^{(r-1)} \times_r \hat{\boldsymbol{L}}_r^{-1}. \tag{7}$$

In (6), $\boldsymbol{U}_r^{(L)}$ and $\boldsymbol{U}_r^{(X)}$ are unitary matrices and $\boldsymbol{\Xi}_r^{(L)}$ and $\boldsymbol{\Xi}_r^{(X)}$ are diagonal matrices, which result from the GSVD of $\left[\widetilde{\boldsymbol{\mathcal{X}}}^{(r)}\right]_{(r)}$ and $\hat{\boldsymbol{L}}$. Since the noise covariance has a Kronecker structure, we can obtain a better estimate of the noise model by considering each $\left[\boldsymbol{\mathcal{N}}^{(\mathrm{c})}\right]_{(i)}$ for $i = 1, 2, \ldots, R+1$. In order to estimate each $\boldsymbol{L}_r$, we calculate the following expression

$$\mathrm{E}\left\{\left[\boldsymbol{\mathcal{N}}^{(\mathrm{c})}\right]_{(r)} \cdot \left(\left[\boldsymbol{\mathcal{N}}^{(\mathrm{c})}\right]_{(r)}\right)^{\mathrm{H}}\right\} = \alpha \cdot \boldsymbol{L}_r \cdot \boldsymbol{L}_r^{\mathrm{H}}. \tag{8}$$

where the proof for (8) is demonstrated in [1]. Note that α is a normalization constant such that $\mathrm{tr}(\boldsymbol{L}_i \cdot \boldsymbol{L}_i^{\mathrm{H}}) = M_i$. Finally, using (8) it is possible to estimate the correlation factor

$\boldsymbol{L}_i$ by applying an eigenvalue decomposition or a Cholesky decomposition.

Assuming that for all $R+1$ dimensions the noise is correlated, the S-GSVD is computed in $R+1$ steps. To initiate the sequential computation of several GSVDs in (6), we set $\widetilde{\boldsymbol{\mathcal{X}}}^{(0)} = \boldsymbol{\mathcal{X}}$. After applying the GSVD for all values of r, we obtain the prewhitened $\widetilde{\boldsymbol{\mathcal{X}}}^{(R+1)}$. Therefore, as shown in [1], we can define the S-GSVD of $\boldsymbol{\mathcal{X}}$ and $\boldsymbol{\mathcal{N}}^{(\mathrm{c})}$ as being

$$\widetilde{\boldsymbol{\mathcal{X}}}^{(R+1)} = \boldsymbol{\mathcal{S}}^{[s]} \times_1 \boldsymbol{U}_1^{[s]} \times_2 \boldsymbol{U}_2^{[s]} \ldots \times_R \boldsymbol{U}_R^{[s]} \times_{R+1} \boldsymbol{U}_{R+1}^{[s]}, \quad (9)$$

where $\boldsymbol{\mathcal{S}}^{[s]} \in \mathbb{C}^{p_1 \times p_2 \ldots \times p_R \times d}$ and $\boldsymbol{U}_r^{[s]} \in \mathbb{C}^{M_r \times p_r}$, such that $p_r = \min(M_r, d)$ for $r = 1, 2, \ldots, R+1$. Note that (9) is equivalent to the HOSVD of the prewhitened tensor $\widetilde{\boldsymbol{\mathcal{X}}}^{(R+1)}$.

Since the subspaces of $\widetilde{\boldsymbol{\mathcal{X}}}^{(R+1)}$ and $\boldsymbol{\mathcal{X}}$ are different, to obtain the same subspace of $\boldsymbol{\mathcal{X}}$ the dewhitening step should be applied in $\widetilde{\boldsymbol{\mathcal{X}}}^{(R+1)}$, where we obtain $\boldsymbol{\mathcal{X}}'$ is given by

$$\begin{aligned} \boldsymbol{\mathcal{X}}' \;=\; & \boldsymbol{\mathcal{S}}^{[s]} \times_1 \left(\hat{\boldsymbol{L}}_1 \cdot \boldsymbol{U}_1^{[s]}\right) \times_2 \left(\hat{\boldsymbol{L}}_2 \cdot \boldsymbol{U}_2^{[s]}\right) \ldots \\ & \times_R \left(\hat{\boldsymbol{L}}_R \cdot \boldsymbol{U}_R^{[s]}\right) \times_{R+1} \left(\boldsymbol{V}_{R+1}^{[s]} \cdot \boldsymbol{\Xi}_{R+1}^{(L)[s]}\right). \end{aligned} \quad (10)$$

Note that $\boldsymbol{\mathcal{X}}' \approx \boldsymbol{\mathcal{X}}$, i.e., a better approximation than using the HOSVD based low-rank truncation, since using the S-GSVD based truncation in (10) the noise structure is taken into account. The accuracy in (10) is improved by computing additionally R SVDs as proposed in [1]. Note that, for notational convenience, we use in (10) $\hat{\boldsymbol{L}}_R \cdot \boldsymbol{U}_R^{[s]}$ instead of $\boldsymbol{V}_R^{[s]} \cdot \boldsymbol{\Xi}_R^{(L)[s]}$ as proposed in [1]. Moreover, the PARAFAC decomposition of $\boldsymbol{\mathcal{X}}'$ can be written as

$$\boldsymbol{\mathcal{X}}' = \boldsymbol{\mathcal{I}}_{R+1,d} \times_1 \hat{\boldsymbol{F}}^{(1)} \times_2 \hat{\boldsymbol{F}}^{(2)} \ldots \times_{R+1} \hat{\boldsymbol{F}}^{(R+1)}, \quad (11)$$

where $\hat{\boldsymbol{F}}^{(r)} = \hat{\boldsymbol{L}}_r \cdot \boldsymbol{U}_r^{[s]} \cdot \boldsymbol{T}_r$ for a nonsingular transformation matrix $\boldsymbol{T}_r \in \mathbb{C}^{d \times d}$ for all modes $r \in \mathcal{R}$, where $\mathcal{R} = \{r | M_r \geq d, r = 1, \ldots, R+1\}$ denotes the set of non-degenerate modes. Therefore, given (11) and since we obtain $\hat{\boldsymbol{L}}_r$ and $\boldsymbol{U}_r^{[s]}$ from the Sequential GSVD [1], we still have to estimate $\boldsymbol{T}_r$ in order to obtain $\hat{\boldsymbol{F}}^{(r)}$. As proposed in [8], the estimation of $\boldsymbol{T}_r$ is performed via simultaneous matrix diagonalizations.

In CFP, several estimates for each factor matrix $\hat{\boldsymbol{F}}^{(r)}$ are returned and one estimate should be selected. In the simulations presented in this paper, we choose the estimates $\hat{\boldsymbol{F}}^{(r)}$ corresponding to the simultaneous diagonalizations with smallest residuals as proposed in [8]. As shown [5], using these estimates of $\hat{\boldsymbol{F}}^{(r)}$ gives estimates of parameters with smallest root mean square error (RMSE). Moreover, each $\hat{\boldsymbol{F}}^{(r)}$ obtained from different simultaneous matrix diagonalizations have a different permutation of the d principal components and in order to make the correct pairing of the permuted main components the amplitude based approach proposed in [12] can be applied.

Up to this point only the estimates $\hat{\boldsymbol{F}}^{(r)}$ are found, however, our objective is to have the estimates $\hat{\mu}_i^{(r)}$. In order to extract the spatial frequencies $\hat{\mu}_i^{(r)}$ from $\hat{\boldsymbol{F}}^{(r)}$, Peak Search (PS) or Shift Invariance (SI) based schemes can be used as proposed in [5]. If the array is shift invariant in the r-th mode, the estimation of the spatial frequency can be performed by exploiting this property as follows

$$\hat{\mu}_i^{(r)} = \arg\left[\left(\boldsymbol{J}_1^{(r)} \cdot \hat{\boldsymbol{f}}_i^{(r)}\right)^{\mathrm{H}} \cdot \boldsymbol{J}_2^{(r)} \cdot \hat{\boldsymbol{f}}_i^{(r)}\right] \quad (12)$$

where the operator $\arg(\cdot)$ returns the phase, and $\boldsymbol{J}_1^{(r)} \in \mathbb{R}^{M_r^{(\mathrm{sel})} \times M_r}$ and $\boldsymbol{J}_2^{(r)} \in \mathbb{R}^{M_r^{(\mathrm{sel})} \times M_r}$ are the selection matrices from the ESPRIT-type algorithms. The selection matrix $\boldsymbol{J}_1^{(r)}$ selects the $M_r^{(\mathrm{sel})}$ elements of the first subarray and the selection matrix $\boldsymbol{J}_2^{(r)}$ selects the $M_r^{(\mathrm{sel})}$ elements of the second subarray [13]. $M_r^{(\mathrm{sel})}$ depends on the geometry of the array, and as an example for the ULA, $M_r^{(\mathrm{sel})} = M_r - 1$ corresponds to maximum overlap.

To increase the maximum model order, with which the CFP is still applicable, pairs of dimensions of the tensor $\boldsymbol{\mathcal{X}}$ can be merged into one dimension as shown in [5]. In order to separate the merged dimensions, a Least Squares Khatri-Rao Factorization (LSKRF) can be applied in conjunction with PS and SI based schemes [5].

IV. Simulation results

In this section, we generate our samples based on the data model of (1), where the spatial frequencies $\mu_i^{(r)}$ are drawn from an uniform distribution in $[-\pi, \pi]$. The source symbols are i.i.d. ZMCSCG distributed with power equal to σ_s^2 for all the sources. The SNR at the receiver is defined as SNR $= 10 \log_{10}\left(\frac{\sigma_s^2}{\sigma_n^2}\right)$, where σ_n^2 is the variance of the elements of the white noise tensor $\boldsymbol{\mathcal{N}}$ in (3). The standard deviation of the positioning error of the array elements in the first and second dimensions is denoted by ρ_e similarly as in [5].

Here we consider that the elements of the noise covariance matrix in the i-th mode $\boldsymbol{W}_i = \boldsymbol{L}_i \cdot \boldsymbol{L}_i^{\mathrm{H}}$ vary as a function of the correlation coefficient ρ_i similarly as in [1]. As an example we consider in (13) the structure of $\boldsymbol{W}_i$ as a function of ρ_i for $M_i = 3$

$$\boldsymbol{W}_i = \begin{bmatrix} 1 & \rho_i^* & (\rho_i^*)^2 \\ \rho_i & 1 & \rho_i^* \\ \rho_i^2 & \rho_i & 1 \end{bmatrix}, \quad (13)$$

where ρ_i is the correlation coefficient. Note that also other types of correlation models can be used. To be consistent with (5), we normalize $\boldsymbol{L}_i$ such that $\mathrm{tr}(\boldsymbol{L}_i \cdot \boldsymbol{L}_i^{\mathrm{H}}) = M_i$.

Similarly to [5], we consider the case that there is a URA with positioning errors at the RX. Therefore, for severe positioning errors, all the distances between all the consecutive antennas are different, which implies that the assumption of an outer product structure between the first and the second dimensions, which are merged in our CFP approach, is not valid anymore. These positioning errors are modeled by zero mean real-valued Gaussian random variables with variance σ_{e}^2. Note that the URA with positioning errors is only included at the RX side, whereas at the TX and frequency dimensions the arrays have a Vandermonde structure without any error. In order to compare the performance of the Sequential

TABLE I
NOTATION OF THE LEGENDS USED IN ALL FIGURES.

Abbreviation	Algorithm
R-D STE w/o PWT	The R-D Standard Tensor-based ESPRIT [2] is applied without prewhitening.
R-D STE S-GSVD	The R-D Standard Tensor-based ESPRIT [2] in conjunction with the S-GSVD II [1] with correlation factors estimation (8) [1] is applied. Note that we include $R-1$ SVDs at the end of the S-GSVD in order to improve the estimation.
CFP-PE	The closed-form PARAFAC parameter estimator is used [5]. In this case, for the parameter extraction, we combine the CFP with the shift invariance scheme according to [5].
S-CFP-PE	The proposed Sequential GSVD based closed-form PARAFAC based parameter estimator combined with the shift invariance scheme is applied.
FBA	This suffix indicates that the Forward Backward Averaging is applied [14], [2] to virtually double the number of samples.
CFP	The closed-form PARAFAC proposed in [8] and modified in [12] is applied.
S-CFP	The proposed Sequential GSVD based closed-form PARAFAC is applied until obtaining $\hat{\boldsymbol{F}}^{(r)}$ and without including the extraction of parameters.

GSVD combined with the closed-form PARAFAC to the other schemes, we compute the root mean squared error (RMSE) of the estimated spatial frequencies $\hat{\mu}_i^{(r)}$ in the third, fourth, and fifth dimensions.

In Table IV, we show the notation used for the schemes presented in all figures. Since for the R-D STE w/o PWT and CFP-PE the colored noise is not taken into account, their performance is severely degraded in comparison to the S-GSVD based schemes as shown in Fig. 2. The R-D STE S-GSVD takes into account the colored noise and similarly as shown in [1] a considerable improvement is achieved compared to the R-D STE w/o PWT. Also as shown in Fig. 2, the S-CFP-PE outperforms the R-D STE S-GSVD, due to the robustness of the closed-form PARAFAC according to [1].

In Fig. 3, by increasing the standard deviation ρ_e of the errors in the arrays of the first and second dimensions, the R-D STE FBA w/o PWT is severely affected due to the FBA, since to apply the FBA a more specific structure is assumed. In this sense, the R-D STE S-GSVD [1] is more robust, since no FBA is applied. However, both ESPRIT-algorithms are outperformed by the closed-form PARAFAC based schemes, S-CFP-PE and CFP-PE. In this case, both schemes have the same performance, since the noise is white.

In general, in Figs. 2 and 3, the performance of R-D STE with FBA is significantly degraded for high values of ρ_e.

In Fig. 4, we vary the SNR and additionally a severely colored noise is assumed for $r = 1, \ldots, 4$. By using the S-GSVD in conjunction with the CFP, the best performance is achieved.

In order to show the applicability of PARAFAC in Kronecker colored noise environments, we compute the relative

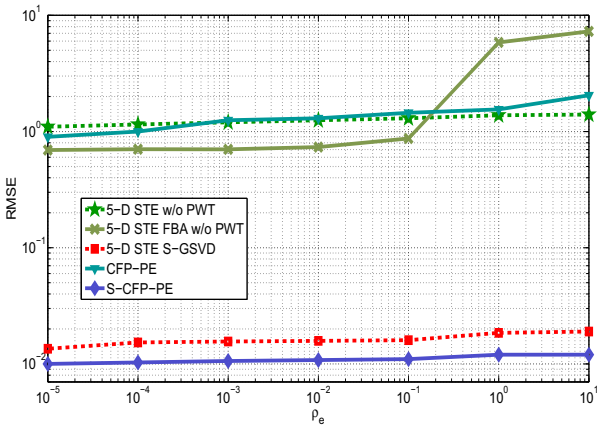

Figure 2. RMSE versus the standard deviation of the array error ρ_e defined in [5] in Kronecker colored environment is depicted. In the simulated scenario, 5 factor matrices have a Vandermonde structure, the array size is $M_1 = 4$, $M_2 = 4$, $M_3 = 4$, $M_4 = 4$, $M_5 = 4$, and $N = 4$, the number of sources $d = 3$, the SNR $= 0$ dB, and the colored noise level $\rho_r = 0.9$ for $r = 1, 2, 3, 4$.

root mean square reconstruction error (rRMSRE) using the CPE and using the S-CFP, which takes the Kronecker structure of the colored noise into account. As in [8], we define the rRMSE as

$$\text{rRMSRE} = \sqrt{\text{E}\left\{ \frac{\left\| \boldsymbol{\mathcal{I}}_{R+1,d} \times_1 \hat{\boldsymbol{F}}^{(1)} \ldots \times_{R+1} \hat{\boldsymbol{F}}^{(R+1)} - \boldsymbol{\mathcal{X}}_0 \right\|_{\text{H}}^2}{\|\boldsymbol{\mathcal{X}}_0\|_{\text{H}}^2} \right\}}, \tag{14}$$

where $\hat{\boldsymbol{F}}^{(r)}$ corresponds to the estimate of $\boldsymbol{F}^{(r)}$. In Fig. 5, for low SNR regimes, an improvement is obtained using the S-CFP instead of the CFP.

The computational complexity of CPE-PE based schemes is much greater than the R-D ESPRIT-type algorithms, since in the closed-form PARAFAC $(R-1) \cdot R$ simultaneous diagonalization problems are solved, while for the R-D ESPRIT-type algorithms only one simultaneous diagonalization is solved. Note that in CFP, several simultaneous diagonalizations (SMDs), i.e., up to $R \cdot (R-1)$ SMDs, can be solved in order to get several estimates for each factor. This information can be used to estimate the model order via the closed-form PARAFAC based model order selection (CFP-MOS) scheme. Solving several SMDs is optional, for a low-complexity version of CFP, already a single SMD can provide estimates for all factors.

V. CONCLUSIONS

In this paper, we propose the Sequential GSVD based closed-form PARAFAC (S-CFP), which is a new PARAFAC decomposition of two tensors, for applications involving colored noise. In contrast to the CFP, which is based on the HOSVD, our proposed scheme takes the colored noise into account, since it is based on the Sequential GSVD (S-GSVD).

For applications related to multidimensional array signal processing [15], the S-CFP based parameter estimator (S-CFP-PE) is applicable to mixed arrays and at the same time

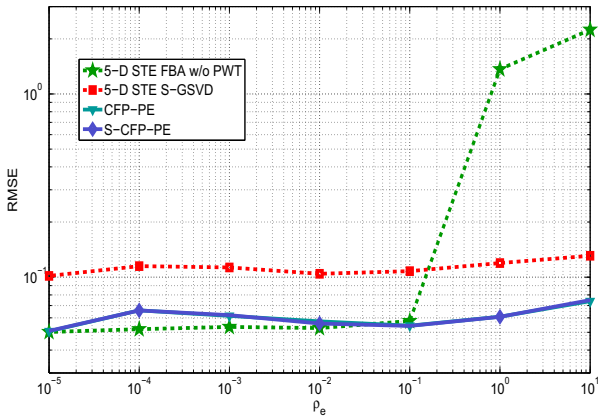

Figure 3. RMSE versus the standard deviation of the array error ρ_e for the case of white and Kronecker colored noise is depicted. In the simulated scenario, R factor matrices have a Vandermonde structure, and the array size is such $R = 5$, $M_1 = 4$, $M_2 = 4$, $M_3 = 4$, $M_4 = 4$, $M_5 = 4$, $N = 4$, and the number of sources $d = 3$. White Gaussian noise is present, i.e., $\rho_r = 0$ for $r = 1, 2, 3, 4$.

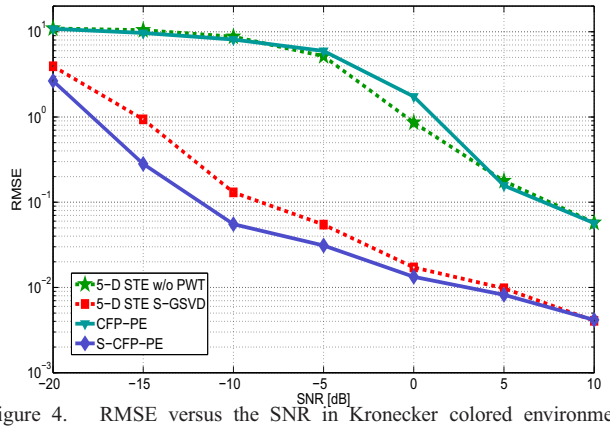

Figure 4. RMSE versus the SNR in Kronecker colored environment is depicted. In the simulated scenario, the array size is $M_1 = 4$, $M_2 = 4$, $M_3 = 4$, $M_4 = 4$, $M_5 = 4$, and $N = 4$, the number of sources $d = 3$, $\rho_e = 1$, and the colored noise level $\rho_r = 0.9$ for $r = 1, 2, 3, 4$.

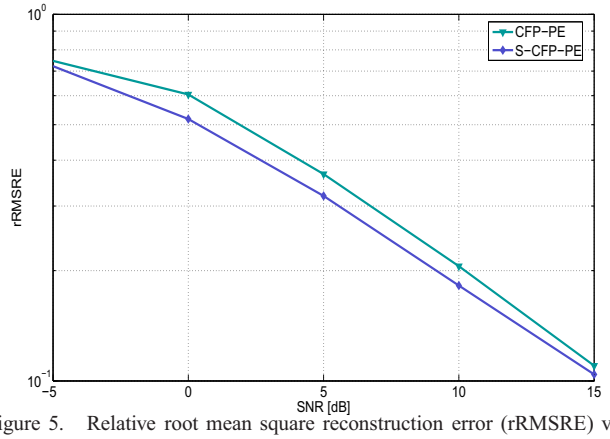

Figure 5. Relative root mean square reconstruction error (rRMSRE) versus the SNR in Kronecker colored environment is depicted. In the simulated scenario, the array size is $M_1 = 4$, $M_2 = 4$, $M_3 = 4$, $M_4 = 4$, $M_5 = 4$, and $N = 4$, the number of sources $d = 3$, and the colored noise level $\rho_r = 0.9$ for $r = 1, 2, 3, 4$.

takes the Kronecker structure of the noise into account. The performance of the S-CFP-PE for low SNR regimes is better than the R-D STE using the S-GSVD, since the S-CFP-PE is more robust against positioning errors in the array.

The reconstruction error is a measure for the accuracy of the decomposition which is independent of its specific structure, such as array steering matrices. The fact that the S-CFP-PE lowers the reconstruction errors suggests that it can be successfully applied for more general problems, such as, those occuring in the food industry [6] and in chemistry [6].

Acknowledgment

The authors thank the International Graduate School on Mobile Communications at the Ilmenau University of Technology.

References

[1] J. P. C. L. da Costa, F. Roemer, and M. Haardt, "Sequential GSVD based prewhitening for multidimensional HOSVD based subspace estimation," in *Proc. ITG Workshop on Smart Antennas*, Berlin, Germany, Feb. 2009.

[2] M. Haardt, F. Roemer, and G. Del Galdo, "Higher-order SVD based subspace estimation to improve the parameter estimation accuracy in multi-dimensional harmonic retrieval problems," *IEEE Transactions on Signal Processing*, vol. 56, no. 7, pp. 3198 – 3213, Jul. 2008.

[3] H. M. Huizenga, J. C. de Munck, L. J. Waldorp, and R. P. P. P. Grasman, "Spatiotemporal EEG/MEG source analysis based on a parametric noise covariance model," *IEEE Transactions on Biomedical Engineering*, vol. 49, no. 6, pp. 533 – 539, Jun. 2002.

[4] B. Park and T. F. Wong, "Training sequence optimization in MIMO systems with colored noise," in *Military Communications Conference (MILCOM 2003)*, Gainesville, USA, Oct. 2003.

[5] J. P. C. L. da Costa, F. Roemer, M. Weis, and M. Haardt, "Robust R-D parameter estimation via closed-form PARAFAC," in *Proc. ITG Workshop on Smart Antennas (WSA'10)*, Bremen, Germany, Feb. 2010.

[6] R. Bro and H. A. L. Kiers, "A new efficient method for determining the number of components in PARAFAC models," *Journal of Chemometrics*, vol. 17, pp. 274–286, 2003.

[7] L. De Lathauwer, B. De Moor, and J. Vandewalle, "A multilinear singular value decomposition," *SIAM J. Matrix Anal. Appl.*, vol. 21(4), 2000.

[8] F. Roemer and M. Haardt, "A closed-form solution for multilinear PARAFAC decompositions," in *Proc. 5-th IEEE Sensor Array and Multich. Sig. Proc. Workshop (SAM 2008)*, Darmstadt, Germany, Jul. 2008, pp. 487 – 491.

[9] J. P. C. L. da Costa, M. Haardt, F. Roemer, and G. Del Galdo, "Enhanced model order estimation using higher-order arrays," in *Proc. 40th Asilomar Conf. on Signals, Systems, and Computers*, Pacific Grove, CA, USA, Nov. 2007.

[10] J. P. C. L. da Costa, M. Haardt, and F. Roemer, "Robust methods based on HOSVD for estimating the model order in PARAFAC models," in *Proc. IEEE Sensor Array and Multichannel Signal Processing Workshop (SAM'08)*, Darmstadt, Germany, Jul. 2008.

[11] J. P. C. L. da Costa, F. Roemer, and M. Haardt, "Iterative sequential GSVD (I-S-GSVD) based prewhitening for multidimensional HOSVD based subspace estimation without knowledge of the noise covariance information," in *Proc. ITG Workshop on Smart Antennas (WSA'10)*, Bremen, Germany, Feb. 2010.

[12] M. Weis, F. Roemer, M. Haardt, D. Jannek, and P. Husar, "Multi-dimensional Space-Time-Frequency component analysis of event-related EEG data using closed-form PARAFAC," in *Proc. IEEE Int. Conf. Acoustics, Speech, and Sig. Proc. (ICASSP 2009)*, Taipei, Taiwan, Apr. 2009.

[13] M. Haardt, "Structured least squares to improve the performance of ESPRIT-type algorithms," *IEEE Transactions on Signal Processing*, vol. 45(3), pp. 792–799, Mar. 1997.

[14] G. Xu, R. H. Roy, and T. Kailath, "Detection of number of sources via exploitation of centro-symmetry property," *IEEE Trans. Signal Processing*, vol. 42, pp. 102–112, Jan. 1994.

[15] J. P. C. L. da Costa, *Parameter Estimation Techniques for Multi-dimensional Array Signal Processing*, 1st ed. Shaker, 2010.